MPC-based Double-Stage Voltage Control of Distribution Networks with High Penetration of Distributed Generation

Zhang, Zhengfa; Silva, Filipe Miguel Faria da; Guo, Yifei; Bak, Claus Leth; Chen, Zhe

Published in:
IECON 2020 The 46th Annual Conference of the IEEE Industrial Electronics Society

DOI (link to publication from Publisher):
10.1109/IECON43393.2020.9254601

Publication date:
2020

Document Version
Accepted author manuscript, peer reviewed version

MPC-based Double-Stage Voltage Control of Distribution Networks with High Penetration of Distributed Generation

1st Zhengfa Zhang
Department of Energy Technology
Aalborg University
Aalborg, Denmark
zhf@et.aau.dk

2nd Filipe Faria da Silva
Department of Energy Technology
Aalborg University
Aalborg, Denmark
ffs@et.aau.dk

3rd Yifei Guo
Department of Electrical & Computer Engineeering
Iowa State University
Ames, USA
yfguo.sdu@gmail.com

4th Claus Leth Bak
Department of Energy Technology
Aalborg University
Aalborg, Denmark
clb@et.aau.dk

5th Zhe Chen
Department of Energy Technology
Aalborg University
Aalborg, Denmark
zch@et.aau.dk

***Abstract*—This paper presents a double-stage voltage control method based on model predictive control to address the voltage regulation in distribution network with high penetration of distributed generation. In the first stage, the operation times of transformer with on-load tap changer and switchable capacitor banks are minimized in hourly timescale. In the second stage, the controller minimizes the distributed generation curtailment while guaranteeing bus voltages within allowed limits with a control period of 1 min. In this paper, an analytical method is applied to calculate the voltage sensitivities with respect to power injections and tap changes. Numerical simulations of a modified IEEE-33 bus system are performed to validate the proposed method.**

***Index Terms*—Voltage control, distribution network, distributed generation, model predictive control**

I. Introduction

In recent years, with the development of renewable energy technology, a growing proportion of distributed generation (DG) based on renewable energy is integrated into distribution networks (DNs) [1]. Unlike traditional large power plants, DG usually has small capacity, rapidly response time and is connected to power grid via power electronic interface. The increased penetration of DG, together with the intermittent and uncertain nature of renewable energy, brings a number of technical challenges to network secure and reliable operation [2]. Voltage regulation problem is one of the most serious among these challenges [3].

Traditional DNs carry electricity from transmission networks to end users. The one-way power flow ensures the voltages at the downstream feeder are usually lower than that at the upstream. However, the reversed power flow caused by high DG production will result in voltage rise problem. Apart from this, the intermittent and uncertain DG output could also lead to larger voltage variation. Currently, distributed system operators (DSOs) mainly rely on operation of transformer with on-load tap changer (OLTC) and capacitor banks (CBs) to control voltages within safe margins. Although these traditional measures are proven by practice to be effective in regulating voltages of traditional feeders, it is recognised that they will no longer sufficient for voltage control of DNs with high penetrated renewable based DG [4]. In addition, the frequent operation of mechanical devices also accelerates their aging process [1]. In [5]–[7], the reactive power outputs of DG are adjusted to improve the voltage profile. But the active power control also plays an important role in voltage regulation due to the high R/X ratio in DNs. Usually, DG is operated at maximum power point tracking (MPPT) mode, it is reasonable when the amount the installed DG is not large. But for DNs with high penetration of DGs, it is no longer appropriate that all DGs operate at MPPT mode, certain amount of active power need to be curtailed to maintain the voltage level within allowed range, especially when having peak generation from DGs. [8] considers a generation curtailment methodology to meet voltage constraints, but its coordination with traditional means, OLTC and CBs, is ignored. In [9] an autonomous curtailment control scheme is proposed in planning stage, but the optimum is not guaranteed with the autonomous control. Based on control rules and optimization, [10] presents a coordinated voltage control scheme to achieve active voltage control, but the control rules become complex with increased number of controllable units. What's more, all above studies

This work is supported by China Scholarship Council and Department of Energy Technology, Aalborg University.

mainly focused on one step optimization, neglecting the relation between two states and also the system future behaviour, which is insufficient to deal with time-variant renewable DG.

Model predictive control (MPC) or receding horizon control has recently received attention in this field [3], [11].The core idea of MPC is to predict the future behaviour of the controlled system over a finite horizon while ensuring certain system constraints [12]. Therefore, MPC is suitable to address above mentioned issue. This paper proposes a double-stage voltage control scheme to realize the coordination of traditional voltage control and DG power outputs. The main contributions of this paper are summarized as follows:

- A double-stage coordinated voltage control method based on MPC is proposed. In the proposed scheme, traditional control devices are regulated at first stage in an hourly timescale and the rapidly response DG is controlled at second stage with control period in minutes.
- An analytical method is adopted to calculated voltage sensitivity coefficients with respect to power injections and OLTC tap changes.
- The proposed method can regulate the voltage profile within allowed range while ensuring the minimum active power curtailed. The performance of the proposed method are validated by numerical simulation of a modified IEEE-33 bus system.

The remainder of this paper is organized as follows. Section II briefly describes system modelling. Section III introduces the formulation of the proposed algorithm. Simulation results are presented in Section IV followed by conclusions.

II. System Modelling

A. Model of Distribution Network

Consider a DN with $N+1$ buses indexed with $i = 0,1,2...N$. As today most DNs are radial and connected to transmission network at the point of common coupling(PCC), let the bus indexed 0 denotes the PCC and assumed to be the reference voltage, the remaining N buses are treated as PQ node. For bus i, let V_i and θ_i denote its voltage magnitude and voltage angle, and defining the corresponding bus voltage vector $\boldsymbol{V} = [V_1\ V_2 \ldots V_N]^T$ and bus voltage angle vector $\boldsymbol{\theta} = [\theta_1\ \theta_2 \ldots \theta_N]^T$. Let P_i, Q_i denote the bus active power and reactive power and they are collected to vectors $\boldsymbol{P} = [P_1\ P_2 \ldots P_N]^T$ and $\boldsymbol{Q} = [Q_1\ Q_2 \ldots Q_N]^T$ respectively. Here we define $\Delta\boldsymbol{V} = \boldsymbol{V}(t) - \boldsymbol{V}(t-1)$ and $\Delta\boldsymbol{\theta} = \boldsymbol{\theta}(t) - \boldsymbol{\theta}(t-1)$ as the vector denoting the small variation of voltage magnitude and voltage angle between time t and $t-1$. The variations of active and reactive power injection are defined as $\Delta\boldsymbol{P}$ and $\Delta\boldsymbol{Q}$ respectively, the Jacobian matrix is denoted as $\boldsymbol{J}$. Then

$$\begin{bmatrix} \Delta\boldsymbol{P} \\ \Delta\boldsymbol{Q} \end{bmatrix} = \boldsymbol{J} \cdot \begin{bmatrix} \Delta\boldsymbol{\theta} \\ \Delta\boldsymbol{V} \end{bmatrix} = \begin{bmatrix} \boldsymbol{H} & \boldsymbol{N} \\ \boldsymbol{K} & \boldsymbol{L} \end{bmatrix} \begin{bmatrix} \Delta\boldsymbol{\theta} \\ \Delta\boldsymbol{V} \end{bmatrix} \tag{1}$$

where

$$\boldsymbol{H} = \left[\frac{\partial P_i}{\partial \theta_j}\right], \boldsymbol{N} = \left[\frac{\partial P_i}{\partial V_j}\right], \boldsymbol{K} = \left[\frac{\partial \mathrm{Q}_i}{\partial \theta_j}\right], \boldsymbol{L} = \left[\frac{\partial \mathrm{Q}_i}{\partial V_j}\right],$$

B. Model of Distributed Generation

DG is connected to power system via power electronic converter interface [13]. So the modelling of DG is as follows:

$$0 \leqslant P_{DG} \leqslant P_{DG}^{max} \tag{2a}$$
$$Q_{DG}^{min} \leqslant Q_{DG} \leqslant Q_{DG}^{max} \tag{2b}$$
$$|\Delta P_{DG}| \leqslant \Delta P_{DG}^{max} \tag{2c}$$
$$|\Delta Q_{DG}| \leqslant \Delta Q_{DG}^{max} \tag{2d}$$
$$\sqrt{P_{DG}^2 + Q_{DG}^2} \leqslant S_{DG} \tag{2e}$$

where S_{DG} is the DG nominal capacity. P_{DG}, Q_{DG} are the DG active power and reactive power output, P_{DG}^{max} and $Q_{DG}^{max}$is DG maximum active and reactive power, ΔP_{DG} and ΔQ_{DG} denote the ramping limit of DG active and reactive power output respectively.

C. Model of OLTC transformer

The OLTC transformer is usually equipped with automatic voltage regulator to control the secondary bus voltage by actions of on load tap changer. Relationship between primary and secondary voltages and limits on tap position actions are expressed as:

$$N_{Tap}^{min} \leqslant N_{Tap} \leqslant N_{Tap}^{max} \tag{3a}$$
$$\Delta N_{Tap}^{min} \leqslant \Delta N_{Tap} \leqslant \Delta N_{Tap}^{max} \tag{3b}$$
$$\frac{V_{sec}}{V_{pri}} = (1 + N_{Tap} \cdot \Delta V_{Tap}) \cdot \frac{V_{N2}}{V_{N1}} \tag{3c}$$

where N_{Tap} and ΔN_{Tap} are tap position and change step of tap position. V_{pri} and V_{sec} are the primary and secondary voltage of the transformer. V_{N1} and V_{N2} are the nominal voltage of primary and secondary side of the transformer. ΔV_{Tap} is the voltage step per tap.

D. Model of Capacitor Bank

The CB can be connected to, or disconnected from the networks by controllable switches. And in this paper, CB is modelled as reactive power sources by including integer number to present the discrete nature [14].

$$Q_{CB} = N_{CB} \cdot q_{CB} \tag{4a}$$
$$N_{CB}^{min} \leqslant N_{CB} \leqslant N_{CB}^{max} \tag{4b}$$
$$|\Delta N_{CB}| \leqslant \Delta N_{CB}^{max} \tag{4c}$$

where q_{CB} is the reactive capacity of each capacitor bank unit, Q_{CB} is the reactive power injection of CB, N_{CB} is the discrete number.

III. Formulation of the Proposed Algorithm

Given the fact that the response speed of traditional voltage control devices is relatively slower than that of DG, the voltage control objective is decomposed into two sub-tasks: the number of action of OLTC and CB is minimized at upper stage with hourly time scale, and the dispatch of DG is controlled at lower stage with shorter time scale of minutes. Before the formulation of proposed algorithm, an analytical voltage sensitivity coefficients calculation method is introduced.

A. Calculation of Voltage Sensitivity Coefficients

Voltage sensitivity describes the dependence between voltage variation $\Delta \boldsymbol{V}$ and $\Delta \boldsymbol{\theta}$ and the change of bus power injections $\Delta \boldsymbol{Q}$ and $\Delta \boldsymbol{P}$. Voltage sensitivity can be obtained by the inverse of Jacobian matrix. But this method has shortcomings: 1) it cannot calculate voltage sensitivity to slack bus voltage and OLTC tap change. 2) The computation burden is large because of invert of high dimensional Jacobian matrix. So the analytical sensitivity calculation method presented in [15] is adopted in this paper to overcome above shortcomings.

1) *voltage sensitivity coefficients with respect to power injections*: Defining $\overline{V_i} \triangleq V_i e^{j\theta_i}$ and $\overline{S_i} = P_i + jQ_i$. The relationship between bus voltages and power injections is:

$$\underline{S_i} = \underline{V_i} \sum_{j=0}^{N} \overline{Y}_{bus,ij} \overline{V_j} \tag{5}$$

where $\underline{S_i}$ and $\underline{V_i}$ are conjugates of $\overline{S_i}$ and $\overline{V_i}$ respectively. $\overline{Y}_{bus}$ denotes the admittance matrix. The partial derivative of bus i voltage magnitude to power injection of bus j can be calculated as follows [15]:

$$\frac{\partial V_i}{\partial P_j} = \frac{1}{V_i} Re\left(\underline{V_i} \frac{\partial \overline{V_i}}{\partial P_j}\right), \; \frac{\partial V_i}{\partial Q_j} = \frac{1}{V_i} Re\left(\underline{V_i} \frac{\partial \overline{V_i}}{\partial Q_j}\right) \tag{6}$$

2) *voltage sensitivity coefficients with respect to tap position*: To calculate voltage sensitivity coefficients with respect to tap position, the voltage sensitivity coefficients with respect to slack bus voltage are firstly derived. For voltage magnitude V_i of bus i, the partial derivative with respect to slack bus voltage magnitude V_k are denoted as:

$$-\overline{V_i} \overline{Y}_{bus,ij} e^{j\theta_k} = \underline{W_{ik}} \sum_{j=0}^{N} \overline{Y}_{bus,ij} \overline{V_j} + \underline{V}_i \sum_{j=1}^{N} \overline{Y}_{bus,ij} \overline{W_{jk}} \tag{7}$$

where

$$\overline{W_{ik}} = \frac{\partial \overline{V_i}}{\partial V_k} = \left(\frac{1}{V_i} \frac{\partial V_i}{\partial V_k} + j \frac{\partial \theta_i}{\partial V_k}\right) \overline{V_i} \tag{8}$$

Then the voltage sensitivity coefficients with respect to slack bus voltage magnitude can be obtained by:

$$\frac{\partial V_i}{\partial V_k} = V_i Re\left(\frac{\overline{W_{ik}}}{\overline{V_i}}\right) \tag{9}$$

Combining (3c) and (9), the voltage sensitivity coefficients with respect to tap changes can be obtained by,

$$\frac{\Delta V_i}{\Delta N_{Tap}} = V_{pri} \cdot \Delta V_{Tap} \cdot \frac{V_{N2}}{V_{N1}} \cdot \frac{\partial V_i}{\partial V_k} \tag{10}$$

B. MPC Principle

The main principle of MPC is illustrated in Fig. 1. MPC uses the current state of the controlled system and solve a finite horizon optimal control problem, while ensuring given system constraints and minimizing a certain cost function. The first move of the calculated optimal control sequence is applied to the controlled system. The control action is changed at the beginning of the control period and maintained within this control period. At next control period, the horizon is shifted and the same process is repeated again [12].

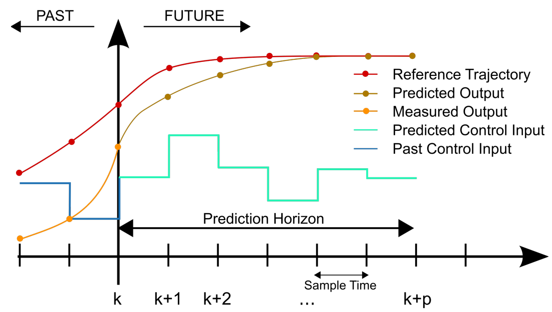

Fig. 1. MPC principle

C. Upper Stage Control

The main objective of upper stage control is to minimize number of OLTC and CB operations to prolong their lifetime. So the upper stage controller is used to minimize the times of action of OLTC and CB while maintain bus voltages close to voltage reference. So the upper stage controller is designed as follows:

$$minimize \sum_{k=1}^{N_P^u} \begin{pmatrix} \omega_V \cdot \|V(k) - V_{ref}\|^2 \\ +\omega_{Tap} \cdot \|Tap(k) - Tap(k-1)\|^2 \\ +\omega_{CB} \cdot \|N_{CB}(k) - N_{CB}(k-1)\|^2 \end{pmatrix} \tag{11}$$

subject to:

$$\boldsymbol{V}(k) = \boldsymbol{V}(k-1) + \frac{\partial \boldsymbol{V}}{\partial \boldsymbol{N}_{Tap}^T} \cdot \Delta \boldsymbol{N}_{Tap}(k-1) + \frac{\partial \boldsymbol{V}}{\partial \boldsymbol{N}_{CB}^T} \cdot \Delta \boldsymbol{N}_{CB}(k-1) \tag{12a}$$

$$\boldsymbol{N}_{tap}^{min} \leqslant \boldsymbol{N}_{Tap}(k) \leqslant \boldsymbol{N}_{tap}^{max}, \; \forall k \tag{12b}$$

$$\Delta \boldsymbol{N}_{tap}^{min} \leqslant \Delta \boldsymbol{N}_{Tap}(k) \leqslant \Delta \boldsymbol{N}_{tap}^{max}, \; \forall k \tag{12c}$$

$$\boldsymbol{N}_{CB}^{min} \leqslant \boldsymbol{N}_{CB}(k) \leqslant \boldsymbol{N}_{CB}^{max}, \; \forall k \tag{12d}$$

$$\Delta \boldsymbol{N}_{CB}^{min} \leqslant \Delta \boldsymbol{N}_{CB}(k) \leqslant \Delta \boldsymbol{N}_{CB}^{max}, \; \forall k \tag{12e}$$

In (11), the first term is used to control bus voltages close to voltage reference, the second and third term is to minimize the number of OLTC and CBs operations. N_P^u is the prediction step of upper stage, V_{ref} is the voltage reference and is chosen as 1.0 pu here. ω_V, ω_{Tap} and ω_{CB} are the weighting factors corresponding to the three terms. (12a) is used to predict the bus voltage of next prediction step according the bus voltage of current step and OLTC and CBs operations, $\partial \boldsymbol{V} / \partial \boldsymbol{N}_{Tap}^T$ and $\partial \boldsymbol{V} / \partial \boldsymbol{N}_{CB}^T$ are voltage sensitivity matrix with respect to OLTC tap change and CB position. $\boldsymbol{N}_{Tap}$ and $\boldsymbol{N}_{CB}$ are OLTC and CB tap positions, $\Delta \boldsymbol{N}_{Tap}$ and $\Delta \boldsymbol{N}_{CB}$ are their step change limit respectively.

D. Lower Stage Control

With high penetration of DG, it's often the case that it not possible to regulate bus voltages within allowed range merely relying on traditional control devices in the upper stage. Thus the bus voltages violating operation limit are compensated by properly dispatching the DG active power and reactive power output. The main objective of lower stage control is to regulate bus voltages into allowed range while minimize the active power curtailed. Note that there is also a cost for reactive power supply by DG [16], so a second term is used to penalty this. The object function of lower stage controller is defined as follows:

$$minimize \sum_{k=1}^{N_p^l} \left(\begin{array}{c} \omega_P \cdot \| \boldsymbol{P}_{DG}^{avi}(k) - \boldsymbol{P}_{DG}(k) \|^2 \\ + \omega_Q \cdot \| \boldsymbol{Q}_{DG}(k) \|^2 \end{array} \right) \tag{13}$$

subject to:

$$\boldsymbol{V}(k) = \boldsymbol{V}(k-1) + \frac{\partial \boldsymbol{V}}{\partial \boldsymbol{P}_{DG}^T} \cdot \boldsymbol{\Delta P}_{DG}(k-1) + \frac{\partial \boldsymbol{V}}{\partial \boldsymbol{Q}_{DG}^T} \cdot \boldsymbol{\Delta Q}_{DG}(k-1) \tag{14a}$$

$$\boldsymbol{V}_{min} \leqslant \boldsymbol{V}(k) \leqslant \boldsymbol{V}_{max}, \forall k \tag{14b}$$

$$\sqrt{P_{DG}(k) + Q_{DG}(k)} \leqslant S_{DG}, \forall k \tag{14c}$$

$$P_{DG}(k) \leqslant P(k)_{DG}^{avi}, \forall k \tag{14d}$$

In (13), the first term is used to penalize the curtailment of active power, the second term denotes the cost for reactive power. N_p^l denotes the prediction step of lower stage control, ω_P and ω_Q are weighting factors for active power curtailment and reactive power production. As the main objective of lower stage controller is to minimize active power curtailment, ω_Q is chosen as much smaller than ω_P. (14a) is used to predict the bus voltage of next step due to DG active power and reactive power injections. $\partial \boldsymbol{V}/\partial \boldsymbol{P}_{DG}^T$ and $\partial \boldsymbol{V}/\partial \boldsymbol{Q}_{DG}^T$ are voltage sensitivity matrix with respect to DG active and reactive power output. $\boldsymbol{V}_{min}$ and $\boldsymbol{V}_{max}$ are voltage limits. As the control period is much longer than that of power electronics converter (in milliseconds), the ramping limit is omitted here.

IV. Case Study

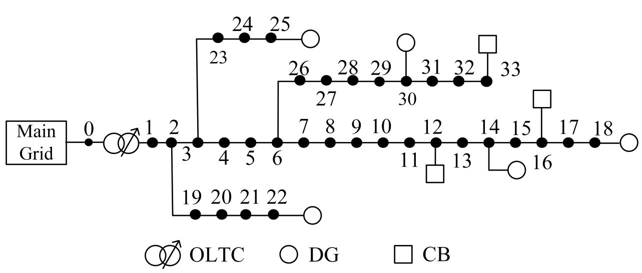

Fig. 2. Topology of Modified IEEE-33 Bus System

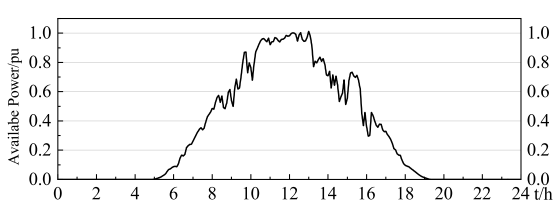

Fig. 3. DG Available Output

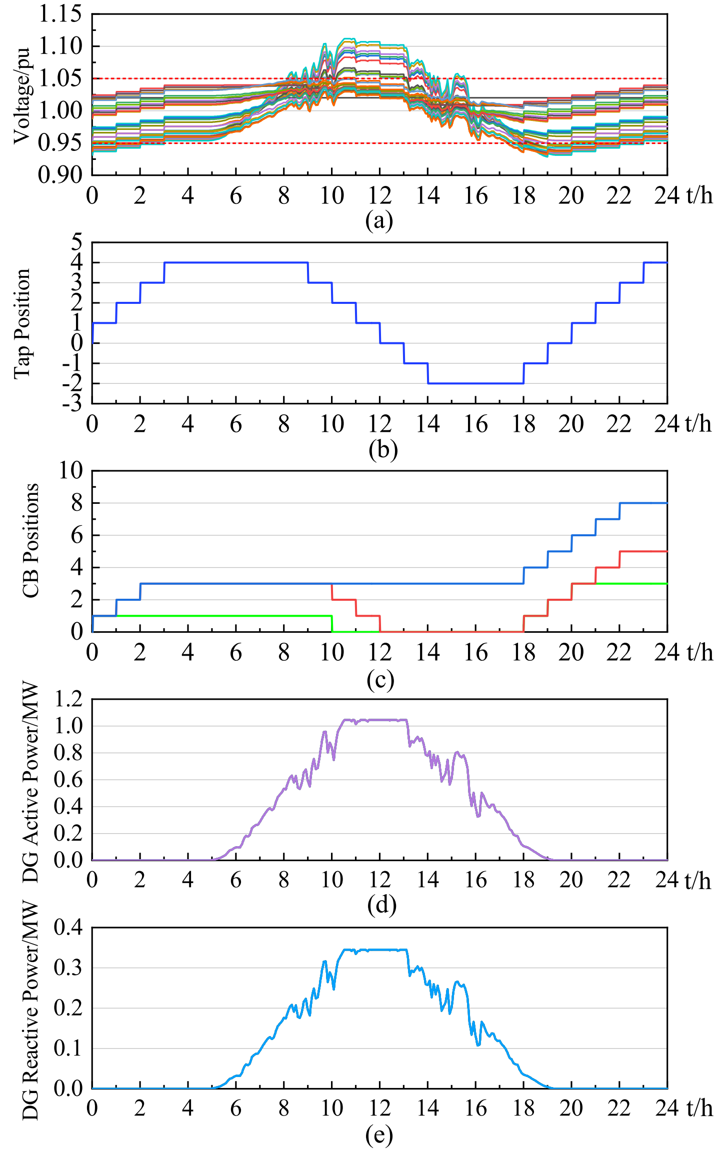

Fig. 4. Simulation Results in Traditional Control

The comparison between traditional voltage control method and proposed voltage control method is presented in this section. The numerical simulation is tested on a modified IEEE-33 bus system, the topology of which is shown in Fig. 2, and model parameter can be found in [17]. The simulation is performed on Matlab r2019b with YALMIP Toolbox [18], and the MPC optimization is solved by Gurobi solver [19]. The time-series DG available output is obtained from the National Renewable Energy Laboratory (NREL) Renewable Resource Data Center [20]. The normalized available output is shown in Fig. 3. In the test system, the voltage of the reference bus is set as 1.02 pu, the maximum and minimum voltage limit are set as 1.05 pu and 0.95 pu respectively. The OLTC has a ±5% tap range with 20 tap positions, so ΔV_{Tap}=0.005, Tap_{min}=-10 and Tap_{max}=10. The DGs are installed at bus 14, 18, 22, 25, 30, each with capacity of 1.1 MVA. The switchable CBs

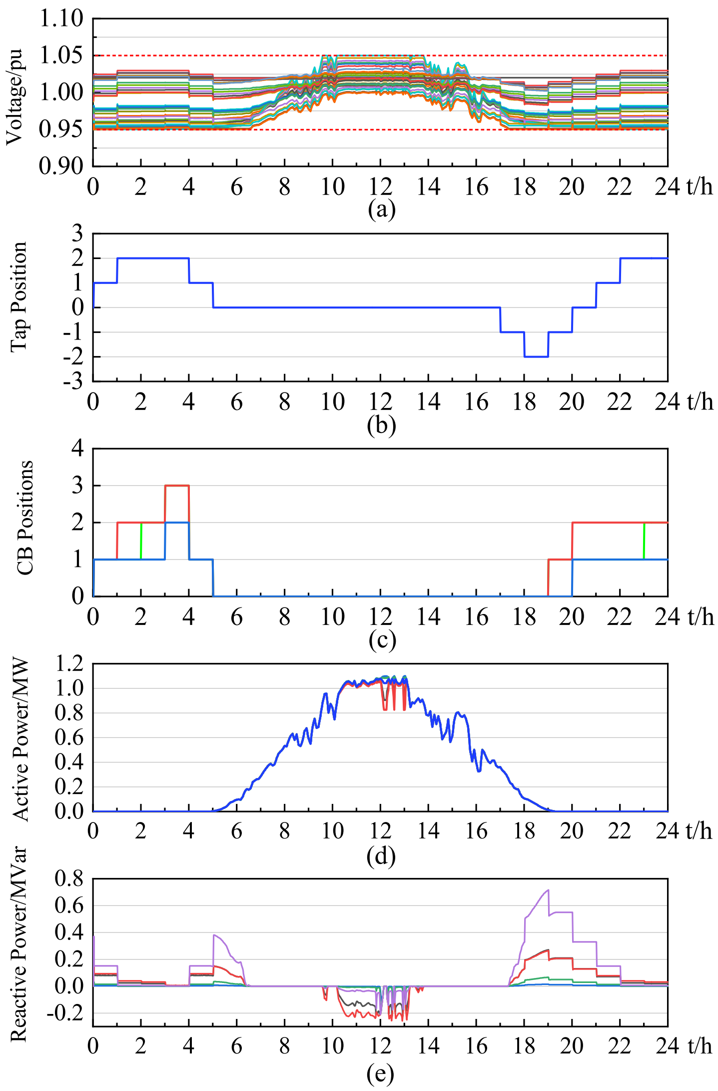

Fig. 5. Simulation Results of the Proposed Control

are located in bus 12, 16, 33, each with capacity of 0.3 MVar and 10 positions. The prediction step for upper stage control and lower stage control is set as 5 and 60 respectively. In traditional control, feeder voltages are controlled relying on operation of OLTC and CBs, DGs follows MPPT mode and are required to operate at a fixed power factor [21], the power factor is chosen as leading power factor of 0.95 here.

The simulation results of two control methods are shown in Fig. 4 and Fig. 5 respectively. As can be seen in Fig. 4, during 0:00-4:00 and 18:00-24:00, when DGs have small output, the overall voltage level is relatively low. In this condition, the voltage profile is mainly controlled by adjustment of OLTC tap position and CBs postions. Traditionally DGs are operated at MPPT, during 8:00-15:00, voltages of certain buses violates the upper limit due to the increasing DG power injection. The most severe time occurs between 11:00 and 13:00 with maximum voltage magnitude of 1.11 pu. But the minimum voltage will fall below 0.93 pu during idle hour.

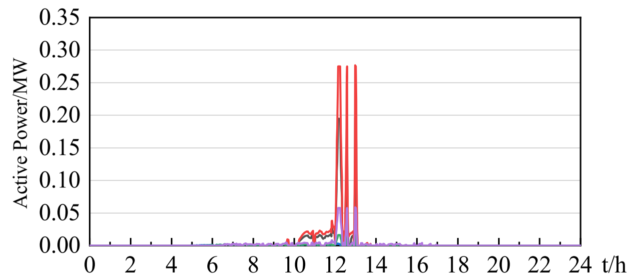

Fig. 6. Curtailments of DG Active Power

Also the OLTC and CBs need to operate frequently in order to regulate the bus voltages. In the whole time range, OLTC operates 15 times with tap position varying between 4 and -2. And the three CBs operate 21 times totally in this period. Traditional method are not effective in regulating bus voltage in this case even though OLTC and CBs frequently operates, demonstrating this method are not suitable for the scenario with high penetration of DGs.

In the simulation results of the proposed method as shown in Fig. 5, the voltage profile is successfully regulated into allowed range by coordination of upper stage and lower stage control. During 0:00-6:00 and 17:30-24:00, OLTC and CBs slightly adjust their positions to raise the overall voltage level, at the same time DGs inject certain amount of reactive power to the distribution grid to support bus voltages. Furthermore, during the most severe time when DGs have maximum output, DGs are required to absorb reactive power instead of injecting reactive power to reduce voltage, meanwhile, certain amount of available active power of some DG units is inevitably curtailed in order to maintain the voltage in the feasible range. As shown in Fig. 6, the maximum curtailed active power of DG located in bus 14 and 18 is 0.19MW and 0.27MW while curtailed active power of other DGs are negligible, demonstrating the proposed method guarantee that the active power curtailed are controlled in the minimum level. In addition, the number of operation of OLTC transformer and CBs are 9 and 15, which reduced by 40% and 28.6% compared with traditional method. The proposed method can achieve flexible coordination between traditional mechanical devices and DG units, overcome the shortcomings of traditional method. The number of OLTC and CBs operation is significantly reduced thus prolonging their lifetime, and the voltage profile is much improved while ensuring maximum power capture. So the proposed control method is more suitable for DN with high penetration of DGs.

V. Conclusion

In this paper, a double stage voltage control method based on MPC is proposed to address the voltage rise problem in DN with high penetration of DG. In the proposed method, the OLTC transformer and capacitor banks are controlled in the upper stage with control period of one hour, while the DG reactive power and active power output are dispatched in 1 min in the lower stage. Numerical simulation demonstrates that proposed method can effectively regulate bus voltages while ensuring the maximum power capture.

REFERENCES

[1] N. Mahmud and A. Zahedi, "Review of control strategies for voltage regulation of the smart distribution network with high penetration of renewable distributed generation," *Renewable and Sustainable Energy Reviews*, vol. 64, pp. 582–595, 2016.

[2] Z. Li and Y. Xu, "Temporally-coordinated optimal operation of a multi-energy microgrid under diverse uncertainties," *Applied energy*, vol. 240, pp. 719–729, 2019.

[3] Y. Guo, Q. Wu, H. Gao, X. Chen, J. Østergaard, and H. Xin, "Mpc-based coordinated voltage regulation for distribution networks with distributed generation and energy storage system," *IEEE Transactions on Sustainable Energy*, vol. 10, no. 4, pp. 1731–1739, 2018.

[4] M. H. Bollen and F. Hassan, *Integration of distributed generation in the power system*. John wiley & sons, 2011, vol. 80.

[5] A. Boynuegri, B. Vural, A. Tascikaraoglu, M. Uzunoglu, and R. Yumurtacı, "Voltage regulation capability of a prototype static var compensator for wind applications," *Applied Energy*, vol. 93, pp. 422–431, 2012.

[6] S. N. Salih and P. Chen, "On coordinated control of oltc and reactive power compensation for voltage regulation in distribution systems with wind power," *IEEE Transactions on Power Systems*, vol. 31, no. 5, pp. 4026–4035, 2015.

[7] B. A. Robbins and A. D. Domínguez-García, "Optimal reactive power dispatch for voltage regulation in unbalanced distribution systems," *IEEE Transactions on Power Systems*, vol. 31, no. 4, pp. 2903–2913, 2015.

[8] Q. Zhou and J. Bialek, "Generation curtailment to manage voltage constraints in distribution networks," *IET Generation, Transmission & Distribution*, vol. 1, no. 3, pp. 492–498, 2007.

[9] M. Džamarija and A. Keane, "Autonomous curtailment control in distributed generation planning," *IEEE Transactions on Smart Grid*, vol. 7, no. 3, pp. 1337–1345, 2015.

[10] A. Kulmala, S. Repo, and P. Järventausta, "Coordinated voltage control in distribution networks including several distributed energy resources," *IEEE Transactions on Smart Grid*, vol. 5, no. 4, pp. 2010–2020, 2014.

[11] G. Valverde and T. Van Cutsem, "Model predictive control of voltages in active distribution networks," *IEEE Transactions on Smart Grid*, vol. 4, no. 4, pp. 2152–2161, 2013.

[12] D. Q. Mayne, J. B. Rawlings, C. V. Rao, and P. O. Scokaert, "Constrained model predictive control: Stability and optimality," *Automatica*, vol. 36, no. 6, pp. 789–814, 2000.

[13] D. Liu, Y. Wang, F. Deng, Q. Zhang, and Z. Chen, "Zero-voltage switching full-bridge t-type dc/dc converter with wide input voltage range and balanced switch currents," *IEEE Transactions on Power Electronics*, vol. 33, no. 12, pp. 10 449–10 466, 2018.

[14] M. Liu, C. A. Canizares, and W. Huang, "Reactive power and voltage control in distribution systems with limited switching operations," *IEEE Transactions on Power Systems*, vol. 24, no. 2, pp. 889–899, 2009.

[15] K. Christakou, J.-Y. LeBoudec, M. Paolone, and D.-C. Tomozei, "Efficient computation of sensitivity coefficients of node voltages and line currents in unbalanced radial electrical distribution networks," *IEEE Transactions on Smart Grid*, vol. 4, no. 2, pp. 741–750, 2013.

[16] M. Braun, "Reactive power supply by distributed generators," in *2008 IEEE Power and Energy Society General Meeting-Conversion and Delivery of Electrical Energy in the 21st Century*. IEEE, 2008, pp. 1–8.

[17] B. Venkatesh, S. Chandramohan, N. Kayalvizhi, and R. K. Devi, "Optimal reconfiguration of radial distribuion system using artificial intelligence methods," in *2009 IEEE Toronto International Conference Science and Technology for Humanity (TIC-STH)*. IEEE, 2009, pp. 660–665.

[18] J. Löfberg, "Yalmip : A toolbox for modeling and optimization in matlab," in *In Proceedings of the CACSD Conference*, Taipei, Taiwan, 2004.

[19] L. Gurobi Optimization, "Gurobi optimizer reference manual," 2020. [Online]. Available: http://www.gurobi.com

[20] "Renewable resource data center." [Online]. Available: https://www.nrel.gov/grid/solar-resource/renewable-resource-data.html

[21] P. N. Vovos, A. E. Kiprakis, A. R. Wallace, and G. P. Harrison, "Centralized and distributed voltage control: Impact on distributed generation penetration," *IEEE Transactions on power systems*, vol. 22, no. 1, pp. 476–483, 2007.